NUMERICAL MODELING OF THE INTERACTION OF A WATER DROP WITH A STRONG AIR SHOCK WAVE

V. S. Surov and V. M. Fomin UDC 533.6.011.72

In an interaction with a weak shock wave, a drop can be treated as a solid particle. Diffraction of an air shock wave on solids has been studied theoretically and experimentally [1-3]. The deformation of the drop must be considered in order to describe an interaction with a strong shock wave correctly. The processes during the interaction of an incompressible gas flow with deformable drops have been studied theoretically [4-6]. A method to calculate the interaction of a water drop with a plane air shock wave has been suggested [7] in which it is assumed that the drop is flattened in the direction of the flow to an ellipsoid of rotation (a spheroidal condition is also used in [4] and [5]). The action of air [shock] waves on drops of various liquids has been studied experimentally [8-13].

1. Formulation of the Problem; Mathematical Model. Let a drop at rest in the gas be hit by a plane shock wave. In the general case, the motion of the liquid and the surrounding gas is described by the complete Navier–Stokes equations:

$$\begin{gathered}
\frac{\partial\rho}{\partial t}+\nabla\cdot(\rho\mathbf{V})=0,\quad \frac{\partial(\rho\mathbf{V})}{\partial t}+\nabla(\rho\mathbf{V}\cdot\mathbf{V})-\rho\mathbf{g}+\nabla\cdot H_{ij}=0,\\
\frac{\partial e}{\partial t}+\nabla\cdot(e\mathbf{V})+\nabla\cdot\mathbf{q}-\rho\mathbf{g}\cdot\mathbf{V}-\nabla\cdot(H_{ij}\mathbf{V})=0,\\
H_{ij}=-p\delta_{ij}+\mu\left[\left(\frac{\partial u_i}{\partial x_j}+\frac{\partial u_j}{\partial x_i}\right)-\frac{2}{3}\delta_{ij}\frac{\partial u_k}{\partial x_k}\right],\\
e=\rho\left(\varepsilon+\frac{\mathbf{V}\cdot\mathbf{V}}{2}\right),\quad \mathbf{q}=-k\nabla T,\quad p=p(\varepsilon,\rho)
\end{gathered}\tag{1.1}$$

with coupling boundary conditions at the contact surface, whose position is not known a priori, but must be determined during the solution. Here ρ is the density; **V** is the velocity vector; g is the gravity acceleration vector; μ is the dynamic viscosity coefficient; δ_{ij} is the Kronecker delta; p is the pressure; e is the total energy of a unit volume of the material; k is the thermal conductivity; T is the temperature; and t is time. Equation (1.1) is written for each of the interacting materials.

We now examine an approximate solution to the problem. Due to the short time of the interaction process, we will not consider thermal phenomena; moreover, we will neglect the viscosity of the liquid and the gas, and also the force of gravity. In this case, the interaction is described by the Euler equations

$$\begin{gathered}
\frac{\partial\rho_i y^\omega}{\partial t}+\frac{\partial\rho_i u_i y^\omega}{\partial x}+\frac{\partial\rho_i v_i y^\omega}{\partial y}=0,\\
\frac{\partial\rho_i u_i y^\omega}{\partial t}+\frac{\partial\left(\rho_i u_i^2+p\right)y^\omega}{\partial x}+\frac{\partial\rho_i u_i v_i y^\omega}{\partial y}=0,\\
\frac{\partial\rho_i v_i y^\omega}{\partial t}+\frac{\partial\rho_i u_i v_i y^\omega}{\partial x}+\frac{\partial\left(\rho_i v_i^2+p\right)y^\omega}{\partial y}-\omega p=0,\\
\frac{\partial\rho_i e_i y^\omega}{\partial t}+\frac{\partial(\rho_i e_i+p)u_i y^\omega}{\partial x}+\frac{\partial(\rho_i e_i+p)v_i y^\omega}{\partial y}=0,
\end{gathered}\tag{1.2}$$

which are written for plane flow symmetry (ω = 0) and axial flow symmetry (ω = 1; the direction of the normal to the front of the incoming shock wave coincides with the direction of

Chelyabinsk and Novosibirsk. Translated from Prikladnaya Mekhanika i Tekhnicheskaya Fizika, No. 1, pp. 48-54, January-February, 1993. Original article submitted March 5, 1990; revision submitted January 15, 1992.

the Oy axis of symmetry of the drop). Here u and v are components of the velocity vector **V** along the x and y axes; the subscript i takes on the values 1 and 2, which correspond to the gas and liquid, respectively.

Equations (1.2) are considered along with the equations of state of the gas and liquid, which have the form

$$p=(\varkappa_1-1)\rho_1\varepsilon_1,\quad p=(\varkappa_2-1)\rho_2\varepsilon_2+c_{02}^2(\rho_2-\rho_{02}), \tag{1.3}$$

where κ_1 = 1.4; κ_2 = 5.59; c_{02} = 1515 m/sec; and ρ_{02} = 1000 kg/m³.

For a given Mach number of the incoming shock wave ($M = D/c_0$, where D is the propagation velocity of the shock front), the displacement velocity of the gas v_s and its density ρ_s and pressure p_s behind the front are determined from the expressions

$$\frac{v_s}{c_0}=\frac{M^2+\frac{p_0}{\rho_0c_0^2}\left[\sqrt{\left(1+\frac{\rho_0c_0^2}{p_0}M^2\right)^2+\varkappa_1^2-1}-\varkappa_1\right]}{(\varkappa_1+1)M}, \tag{1.4}$$
$$\rho_s=\frac{\rho_0c_0M}{c_0M-v_s},\quad p_s=p_0+\rho_0v_sc_0M,$$

which follows from the Rankine–Hugoniot relationships (c_0 is the sound speed, and the subscript 0 denotes parameters in an unperturbed gas).

By convention, the interaction of the drop with the shock wave can be divided into an initial stage and a basic stage. From the moment the front of the incoming air wave touches the surface of the drop, a shock wave propagates through it. As can be seen from one-dimensional calculations, for example for an air shock with M = 11, the velocity of the shock wave propagating through the drop is equal to 1630 m/sec, and the displacement velocity of the liquid behind the front is 67 m/sec. During the time for the air shock to travel a distance of one drop diameter d_0, the forward part of the drop is displaced by $0.02\cdot d_0$, and the change of the transverse dimension of the drop is $0.01\cdot d_0$ from Burger's theoretical model [9]. From these data it can be seen that, in the initial or "wave" stage, the drop hardly "feels" the effect of the air shock wave. The second stage is more significant; because during this stage the drop accelerates and deforms, due to the nonuniform pressure distribution on the drop surface.

For a more complete representation of the processes which occur during the interaction, we now examine the initial stage of shock wave diffraction in more detail on a spherical drop of a compressible liquid.

When an air shock wave interacts with a spherical liquid drop, a system of compatibility equations describes the flow of the liquid and gas near the point where the incoming shock wave contacts the drop surface in coordinates which move with the contact surface (Fig. 1a):

$$\begin{gathered}
v_{n1}\sin\varphi-c_0M\sin(\alpha+\varphi)=0,\ v_{t1}\sin\varphi-\\
-c_0M\cos(\alpha+\varphi)=0,\\
v'_{t1}\cos(\alpha-\gamma)-v_{t1}\sin(\alpha-\gamma)=0,\quad \rho'_1v'_{n1}-\rho_0v_{n1}=0,\\
p+\rho'_1(v'_{n1})^2-p_s-\rho_sv_{n1}^2=0,\\
\varepsilon'_1+(v'_{n1})^2/2+p/\rho'_1-\varepsilon_s-v_{n1}^2/2-p_s/\rho_s=0,\\
p-(\varkappa_1-1)\rho'_1\varepsilon'_1=0,\quad v_{n2}+v\cos(\beta+\vartheta)=0,\quad v_{t2}+v\sin(\beta+\vartheta)=0,\\
v^2=(c_0M\operatorname{ctg}\varphi)^2+(c_0M-v_s)^2,\ (c_0M-v_s)\operatorname{tg}\vartheta-\\
-c_0M\operatorname{ctg}\varphi=0,\\
v_{n2}\cos(\beta+\gamma)-v_{t2}\sin(\beta+\gamma)=0,\\
\rho'_2v'_{n2}-\rho_{02}v_{n2}=0,\quad p+\rho'_2(v'_{n2})^2-\rho_{02}v_{n2}^2=0,\\
\varepsilon'_2+(v'_{n2})^2/2+p/\rho'_2-\varepsilon_{02}-v_{n2}^2/2-p_0/\rho_{02}=0,\\
p-(\varkappa_2-1)\rho'_2\varepsilon'_2-c_{02}^2(\rho'_2-\rho_{02})=0,
\end{gathered} \tag{1.5}$$

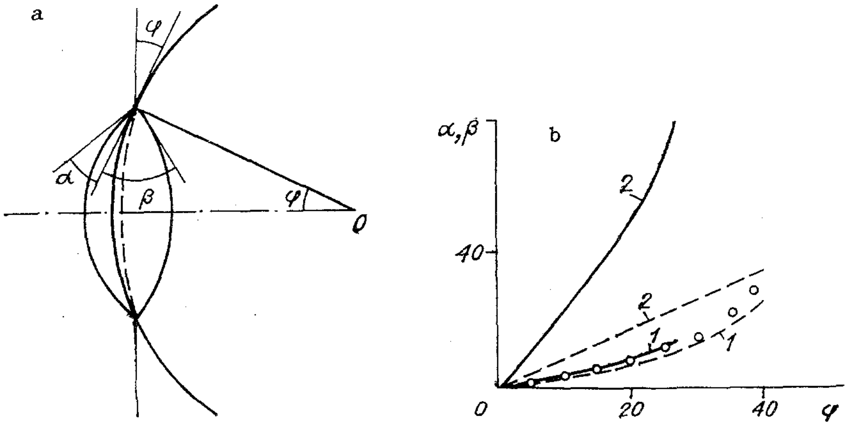

Fig. 1

where the subscripts n and t denote the normal and tangential components of the velocity vectors to the attached shock wave and the primes denote quantities for the reflected and refracted shock waves. In the case of a "rigid" drop, the system of equations (1.5) can be transformed and reduced to the equation

$$\frac{2\varkappa_1 p_s}{\rho_s v_s^2} + \cos(\alpha+\vartheta)\left[(\varkappa_1 - 1)\cos(\alpha+\vartheta) + (\varkappa_1+1)\sin(\alpha+\vartheta)\,\mathrm{tg}(\alpha-\varphi)\right] = 0. \tag{1.6}$$

We now show an approximate method to solve the system (1.5), which substantially simplifies the calculations. For this purpose we make use of the expressions

$$c_0 \mathrm{M}\sin(\alpha+\varphi) - c_1 \sin\varphi = 0,\ c_0\mathrm{M}\sin(\beta-\varphi) - c_2\sin\varphi = 0, \tag{1.7}$$

which relate the inclination angles of the reflected and refracted shock waves to the problem parameters which follow from Huygens principle [14]. We evaluate the propagation velocities c_1 and c_2 of the perturbations from the relationships

$$c_1 \approx \sqrt{c_0^2 + [(\varkappa_1+1)v_s/4]^2} + (\varkappa_1 - 3)v_s/4,\quad c_2 \approx c_{02}.$$

After the angles α and β are calculated from Eqs. (1.7), the other parameters can be calculated explicitly from (1.5). The value of the pressure at the contact point is obtained from the expression

$$p \approx p_s + \rho_s v_{n1}[(v_{n1} - v_{t1})\,\mathrm{tg}(\alpha-\varphi)],$$

which follows from (1.5) and the approximate equality $\gamma \approx \varphi$.

The exact solution of the system of equations (1.5) is obtained by using Newton's iteration method. We note that the approximate solution essentially coincides with the exact solution for the Mach numbers examined.

Figure 1b shows the inclination angles α and β of the connected shock waves (curves 1 and 2) as functions of the contact angle φ for a shock wave with M = 2 (solid curves), which were obtained in the calculations. The circles denote the solution for a "rigid" sphere (M = 2) obtained from (1.6). It can be seen that the drop can be considered "rigid" up to a contact angle $\varphi < \varphi_* \approx 27°$. Here φ_* is the critical angle, that is the maximum angle φ at which a solution to the system of Eqs. (1.5) still exists. We note that φ_* is less than the critical angle φ_{**} for a "rigid" sphere, which separates the regular stage of reflection from the Mach stage. This is related to the fact that for $\varphi > \varphi_*$ the velocity of perturbations, which propagate through the drop, exceeds the velocity of the motion of the contact point between the front of the incoming shock wave and the drop surface; consequently a configuration cannot exist with three shock waves (the incoming, the reflected, and the refracted), which are joined to the contact point. In this case, instead of a refracted shock wave, a rarefaction wave is formed. We note that, due to its large inertia and the small interaction time, the liquid is accelerated only insignificantly in the shock wave, so that

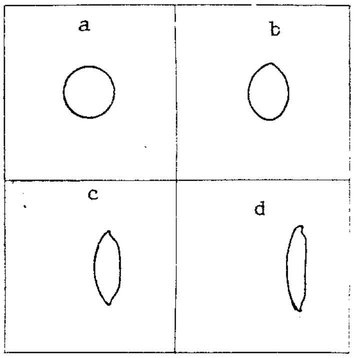

Fig. 2

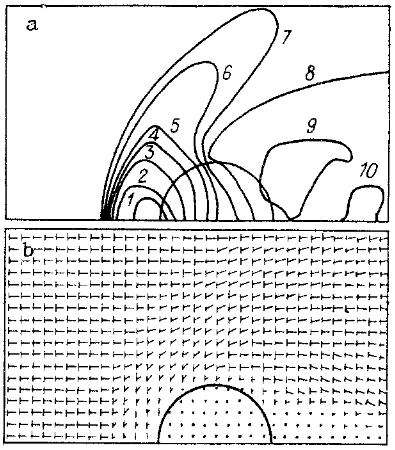

Fig. 3

the drop can also be considered as a solid particle for contact angles exceeding the critical angle.

As M of the incoming shock wave increases, the value of φ_* asymptotically approaches the angle φ_{**} for a "rigid" sphere; starting with M = 3, φ_{**} practically coincides with and tends to a limiting value of ~39°. The dashed curves in Fig. 1b denote the dependences for a shock wave with M = 5.

From this analysis it follows that the liquid compressibility, which must be considered in the wave stage of interaction, turns out not to be that substantial as a whole, so that hereafter the drop is considered incompressible. Thus, the general system of equations (1.1) reduces to two groups of equations: the Euler equations (1.2) for the gas and the Navier–Stokes equations

$$\frac{\partial u y^{\omega}}{\partial x} + \frac{\partial v y^{\omega}}{\partial y} = 0,$$

$$\frac{\partial u y^{\omega}}{\partial t} + \frac{\partial u^2 y^{\omega}}{\partial x} + \frac{\partial u v y^{\omega}}{\partial y} + \nu\left(\frac{\partial^2 u y^{\omega}}{\partial x^2} + y^{\omega}\frac{\partial^2 u}{\partial y^2} + \omega\frac{\partial u}{\partial y}\right) + \frac{y^{\omega}\partial p}{\rho_0\,\partial x} - g_x y^{\omega} = 0, \tag{1.8}$$

$$\frac{\partial v y^{\omega}}{\partial t} + \frac{\partial u v y^{\omega}}{\partial x} + \frac{\partial v^2 y^{\omega}}{\partial y} + \nu\left(\frac{\partial^2 v y^{\omega}}{\partial x^2} + y^{\omega}\frac{\partial^2 v}{\partial y^2} + \omega\frac{\partial u}{\partial y} + \frac{\omega v}{y^{\omega}}\right) + \frac{y^{\omega}\,\partial p}{\rho_0\,\partial y} - g_y y^{\omega} = 0$$

for the drop. Here ν is the kinematic viscosity ($\nu = \mu/\rho_0$); the notation is the same as in (1.1) and (1.2).

2. Numerical Solution. In order to solve the system of equations (1.2), we used Godunov's method [15], and for (1.8) we used the method of [16]. The deformation of the drop was determined by using a modification of the method of markers [16].

Because the gas density is significantly less than the liquid density, simplified boundary conditions were used at the contact boundary. The calculation of each time step of the coupled problem was divided into two stages: first the "external" problem of gas flowing around the drop was solved for a movable surface which was impermeable to the gas; then, from the known external pressure from the first stage, the liquid flow was calculated by considering the contact surface a "free" boundary. From the stability conditions, the allowable time step for the gas was 5-10 times less than that for the liquid; therefore, as a rule, one step for the liquid motion preceded several steps for the gas. This "decomposition" of the boundary conditions made it easy to consider the surface tension as a Laplace correction to the external pressure, which was calculated in the first stage. We note that for the strong shock waves and large drops considered here, the forces from the surface tension are more than an order of magnitude less than the aerodynamic forces and therefore had no substantial effect on the interaction process.

A series of calculations were done for the shock-wave interaction of a water drop with an initial spherical form (d_0 = 2 mm). The Mach number was varied from 3 to 15. Data are presented below for M = 11. The results for other Mach numbers are qualitatively similar.

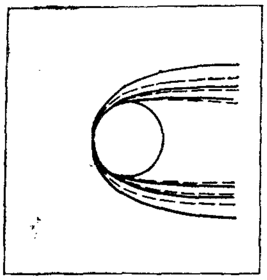

Fig. 4

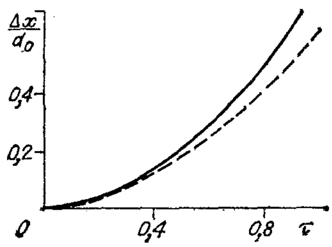

Fig. 5

Figures 2a-2d show the position of the markers which characterize the deformation of the drop at times t = 0, 4.7, 8.7, and 11.5 μsec. It can be seen that over time the drops deform, compress in the direction of the axis of symmetry, and expand in the radial direction.

Figures 3a and 3b show characteristic fragments of the pressure and velocity fields at time t = 1.9 μsec. In Fig. 3a the numbers 10 and 1 denote the isobars with the minimum and maximum pressures (0.02 and 0.53 MPa). It can be seen that the picture of the interaction is close to that for flow around a solid body. An outgoing shock wave also forms ahead of the drop; however, as opposed to [the case of] a solid body, its shape and position change with time due to the drop deformation and acceleration.

Interaction of a drop with a strong shock wave is characterized by breakoff of very fine particles (spray) from the drop surface. The drop appears wrapped by a spray cloud [8-13]. Under these conditions it is rather difficult to determine the actual shape of the drop experimentally. Figure 4 shows trajectories of liquid particles 1 μm and 25 μm in diameter (denoted by dashed and solid lines, respectively), which are broken off from various points of the front surface of the drop. The trajectory problem for known gas dynamic parameters near the drop was solved numerically by integrating a system of ordinary differential equations of motion by the Runga–Kutta method:

$$\frac{du_l}{dt}=\frac{3}{8}\,\frac{c_x\rho_g}{r_k\rho_l}(u_g-u_l)\,|\,u_g-u_l\,|,\quad \frac{dv_l}{dt}=\frac{3}{8}\,\frac{c_y\rho_g}{r_k\rho_l}(v_g-v_l)\,|\,v_g-v_l\,|. \tag{2.1}$$

Here r_k is the particle radius; the subscripts g and ℓ denote the gas and liquid parameters; and the drag coefficients c_x and c_y are calculated from the Henderson equations [17]. The trajectories of the fine particles with a diameter up to 5 μm essentially coincide with the flow lines of the gas. As the diameter of the particles increases, their trajectories become distributed farther from the drop surface, due to their larger inertia. The length of the trajectory from the drop also depends on its initial position at the moment of breakoff.

Figure 5 shows the relative displacement of a drop ($\Delta x/d_0$) along the axis of symmetry as a function of the dimensionless time $\tau = t/t_0$, where $t_0 = d_0 v_S^{-1}\cdot(\rho_2/\rho_S)^{0.5}$. The solid lines describe the curve $\Delta x/d_0 = 0.8\,\tau^2$, which approximates experimental results [8, 13], while the dashed curves are obtained from calculations. A noticeable deviation of the calculated results from the experimental data is observed after time t = 2.9 μsec, which evidently is related to not considering the mass loss of the drop due to "abrasion."

Qualitatively similar results are presented in [18]. Consideration of the drop compressibility places almost overwhelming limitations on the time step; therefore practical results can be obtained only for large Mach numbers. We also note that, as opposed to [18] where the Euler equations (1.2) were used to calculate the liquid motion, there are no zones moving in the negative direction within the drop at any time during the calculation.

LITERATURE CITED

1. V. P. Kolgan and A. S. Fonarev, "Establishing the flow around a cylinder and a sphere from shock wave impact," Izv. Akad. Nauk SSSR, Mekh. Zhidk. Gaza, No. 5 (1972).
2. G. M. Artyunyan and A. V. Karchevskii, Reflected Shock Waves [in Russian], Mashinostroenie, Moscow (1973).
3. G. V. Bazhenova and O. G. Gvozdeva, Transient Interactions of Shock and Detonation Waves in Gases [in Russian], Nauka, Moscow (1986).

4. L. A. Klyachko, "On the theory of drop breakup by a gas flow," Inzh. Zh., 3, No. 3 (1963).
5. M. S. Volynskii and A. S. Lipatov, "Deformation and breakup of drops in a gas flow," Inzh. Fiz. Zh., 18, No. 5 (1970).
6. A. L. Gonor and N. V. Zolotova, "Deceleration and deformation of a liquid drop in a gas flow," Izv. Akad. Nauk SSSR, Mekh. Zhidk. Gaza, No. 2 (1981).
7. V. V. Mitrofanov, "Equations for the deformation of a liquid drop in a gas flow behind a shock wave," in: Dynamics of Continuous Media, No. 39, Collection of Scientific Works of the Russian Academy of Sciences, Siberian Department, Institute of Hydrodynamics (1979).
8. W. G. Reinecke and G. D. Waldman, "An investigation of water drop disintegration in the region behind strong shock waves," Proc. 3rd International Conf., Rain Erosion and Related Phenomena, Hartley-Whitney, Hampshire (1970).
9. A. A. Buzukov, "Disintegration of drops in the stream of an air shock wave," Prikl. Mekh. Tekh. Fiz., No. 2 (1963).
10. A. A. Ranger and J. A. Nicholls, "Aerodynamic shattering of liquid drops," AIAA J., 7, No. 27 (1969).
11. B. E. Gel'fand, S. A. Gubin, and S. M. Kogarko, "Differences in drop breakup in shock waves and their characteristics," Inzh. Fiz. Zh., 27, No. 1 (1974).
12. B. M. Belen'kii and G. A. Evseev, "Experimental investigation of drop disintegration from gas motion behind a shock wave," Izv. Akad. Nauk SSSR, Mekh. Zhidk. Gaza, No. 2 (1974).
13. V. M. Boiko, A. N. Papyrin, and S. V. Poplavskii, "On the dynamics of drop breakup in shock waves," Prikl. Mekh. Tekh. Fiz., No. 2 (1987).
14. M. B. Lesser, "Analytic solution of liquid-drop impact problems," Proc. R. Soc. London, A377, No. 1770 (1981).
15. S. K. Godunov, A. V. Zabrodin, M. Ya. Ivanov, et al., Numerical Solution of Multidimensional Problems of Gas Dynamics [in Russian], Nauka, Moscow (1976).
16. F. H. Harlow and J. P. Shannon, "Numerical calculation of time-dependent viscous incompressible flow with a free surface," Phys. Fluids, 8, No. 12 (1965).
17. N. N. Yanenko, R. I. Soloukhin, A. N. Papyrin, and V. M. Fomin, Supersonic Two-Phase Flow under Conditions of Fast Nonequilibrium Particles [in Russian], Nauka, Novosibirsk (1980).
18. V. S. Surov and S. G. Ageev, "Numerical modeling of the interaction of a spherical water drop in a strong shock wave," in: Modeling and Mechanics [in Russian], Vol. 4(21), No. 3, Academy of Sciences, Siberian Department, Computer Center, Institute of Theoretical and Applied Mechanics (1990).